Article

Journal of
Nanoscience and Nanotechnology
Vol. 14, 1–5, 2014
www.aspbs.com/jnn

Viscoelastic Properties of Poly[(butylene succinate)-co-adipate] Nanocomposites

Shaeel A. Al-Thabaiti[1], Suprakas Sinha Ray[1, 2, *],
Sulaiman Nassir Basahel[1], and Mohamed Mokhtar[1]

[1] *Department of Chemistry, King Abdulaziz University, Jeddah 21589, Kingdom of Saudi Arabia*
[2] *DST/CSIR National Centre for Nanostructured Materials, Council for Scientific and Industrial Research, Pretoria 0001, South Africa*

This article reports the viscoelastic properties of poly[(butylene succinate)-co-adipate] (PBSA) nanocomposites. The nanocomposites of PBSA with various loadings of organically modified clay were prepared by melt-mixing in a batch-mixer. The solid and melt-state viscoelastic properties of neat PBSA and various nanocomposites were studied in detail. The dynamic mechanical studies demonstrated an increase in the storage modulus of PBSA matrix with organoclay loading. Melt-state rheological properties were found to be modified with organoclay loading changing from liquid-like, to gel-like and then viscoelastic solid-like. Such changes in viscoelastic properties along with the improvements in thermomechanical properties are expected to open opportunities for the use of PBSA extending its applications from the classical field of packaging to new niches such as tissue-engineering.

Keywords: Poly[(butylenes succinate)-co-adipate], Nanocomposites, Voiscoelastic Properties.

1. INTRODUCTION

Poly[(butylene succinate)-co-adipate] (PBSA) is a synthetic aliphatic polyester and is synthesized by the polycondensation of butane-1,4-diol in the presence of succinic and adipic acids with relatively low production cost and satisfactory mechanical properties equivalent to that of polyolefins.[1–3] PBSA, compared with poly(butylene succinate), is more susceptible to biodegradation because of its lower crystallinity and more flexible polymer chains.[3] Because of the 'green' feature, it has been proposed as a degradable plastic for uses in service-ware, grocery, waste-composting bags, mulch films, etc.[4] However, mechanical and other properties of PBSA, such as softness, gas-barrier, and thermal stability of the neat polymer are often not sufficient for wide-range of end-use applications.

In recent years, a great effort has been made to develop high-performance novel polymeric materials through the benefit of nanotechnology. One of such niche areas is polymer nanocomposite (PNC) technology.[5–15] By definition, PNCs are really nanofilled plastics, where the total interfacial area becomes the critical characteristic rather than simply the relative volume fraction of constituents. However, the use of the term PNCs invokes parallels to the traditional fiber-reinforced composite technology and the ability to spatially 'engineer, design, and tailor' materials performance for a given application.[16] Recently, PNC technology not only expands the performance space of traditional filled polymers, but also introduces completely new combinations of properties and thus enables new applications for plastics.[16, 17]

Of particular interest is the clay-containing PNC that consists of a polymer and pristine or organically modified clay which often exhibit concurrent improved properties as compared to those of the pure polymer.[18–21] In general, it is believed that these concurrent property improvements in polymer/clay nanocomposite come from the interfacial interactions between the polymer matrix and the clay particles, as opposed to the conventional composites.[21]

In our recent publications in this series,[22–25] we have reported on the preparation, characterization, and mechanical and material properties of various types of PBSA nanocomposites prepared with different types of organically modified clays. In all cases the intrinsic properties of

*Author to whom correspondence should be addressed.

the neat PBSA are concurrently improved after nanocomposites formation. In this article, we report details of the solid- and melt-state viscoelastic properties of PBSA nanocomposites because the measurement of viscoelastic properties of polymeric materials is crucial to gain a fundamental understanding of the structure-property relationship and also the nature of processability for these materials. Aside from these on the basis of viscoelastic behavior under molten state we can easily find out the strength of PBSA/organoclay interactions in the case of nanocomposites.

2. EXPERIMENTAL DETAILS

PBSA used in this study is a commercial product from Showa High Polymer (Japan), with the designation BIONOLLE #3001, which according to the supplier has a weight average molecular weight, $M_w = 190$ kg/mol, specific gravity $= 1.23$ g/cm^3 (ASTMD729), and melt flow index (MFI) $= 1.8$ gm/10 min (190 °C, ASTM1238). The molar ratio of succinate unit to the adipate unit is ~4:1 and the content of the coupling agent (hexamethylene diisocyanate) unit is ~0.5 mol.%. Organoclay used in this study was Cloisite® 30B (C30B), purchased from the Southern Clay Products, USA. According to the supplier, the pristine MMT is modified with 30 wt.% of methyl tallow bis(2-hydroxylethyl) quaternary ammonium salt. The reason for choosing C30B as an OMMT in this study is that it has the closest value of the polar solubility parameter of the surfactant (21.5 $J^{1/2} \cdot cm^{-3/2}$) with that of PBSA (23.8 $J^{1/2} \cdot cm^{-3/2}$).[23] Prior to melt blending, the polymer was dried under vacuum at 60 °C for 48 h and C30B at 75 °C for 4 h.

Since PBSA is a semicrystalline polymer having the highest melting peak temperature at around 95 °C, the selected processing temperature was 125 °C. Nanocomposites of PBSA with various C30B loading were prepared via melt-mixing technique. PBSA was first melted in a Polylab Thermohaake-batch mixer at 125 °C (set temperature) for 1.5 min with a rotor speed of 60 rpm. C30B powder was then added for 1 min and blended for 6.5 min. The dried nanocomposite strands were converted into sheets with a thickness of 0.4–1.5 mm by pressing with 2 torr pressure at 125 °C for 2 min using the Craver Laboratory Press. The PBSA nanocomposites with various wt.% of C30B such as 3, 4, 5, and 6, were correspondingly abbreviated as PBSACN3, PBSACN4, PBSACN5, and PBSACN6.

The degree of dispersion of silicate layers in the PBSA matrix was evaluated by STEM. For the STEM studies, ~75 nm thick compression molded nanocomposite lamellae were prepared using a Focused Ion Beam FEI Helios Nanolab SEM (FIB-SEM) (Gallium ion source and beam current was 0.92 mA), operated at 30 kV. To avoid damage, the sample surface was first covered with a platinum deposition. Details regarding lamella preparation by FIB-SEM can be found elsewhere.[24] Bright-field STEM images of various nanocomposite samples were taken in a FEI Helios Nanolab SEM using STEM-II detector.

The flow behavior of neat PBSA and various nanocomposites in both melt and solid states were studied by an Anton-Paar stress–strain controlled rheometer model MCR-501 with parallel plate (PP-25) configuration and solid rectangular fixture (SRF), respectively. To do the dynamic oscillatory measurements one should first determine the amplitude of oscillation in the linear viscoelastic (LVE) region where any structural change is supposed to be reversible. Hence, the strain amplitude sweep experiments of all samples were performed at 125 °C with a constant angular frequency (ω) $= 6.28$ rad/s in the varying strain window 0.01–100%. The frequency sweep experiments were carried out at the same temperature with a strain amplitude of 0.1% in the frequency range 100–0.01 rad/s. For time sweep experiments, the samples were investigated for 1200 s at a constant temperature of 125 °C, strain $= 0.1\%$ and $\omega = 6.28$ rad/s.

3. RESULTS AND DISCUSSION

The state of dispersion of silicate layers within PBSA matrix was analysed by STEM technique. Several zones of the composites were observed by electron microscopy and the provided micrographs were selected to faithfully represent the overall state of dispersion distribution. Figure 1 shows the bright-field STEM images of various PBSACNs in which black entities represent the dispersed clay layers. The STEM image of PBSACN3 shows that as a whole the clay particles are dispersed nicely in the PBSA matrix and the inter-particle distance is much higher than the other nanocomposites. Still there is some overlapping of neighboring particles, which increases the stacking of the clay layers. In the case of PBSACN4, the dispersion characteristics are almost the same as PBSACN3; however, only the probability of finding neighbors increases. According to the STEM, PBSACN5 has a flocculated structure. Further increase in C30B loading results the formation of stacked-intercalated structure like in the case of PBSACN6. Therefore, the structure of nanocomposites is changing especially from PBSACN4 to PBSACN5 and then in PBSACN6. With increase in C30B loading, clay stacking increases, the flexibility of the samples decreases and they start to behave like solid materials. This type of structural changes will be confirmed by melt-state viscoelastic property measurements.

Dynamic mechanical analyses provide the thermomechanical material response under a periodic stress with variation of time, temperature or frequency of oscillations. The current study focuses on the variation of the G' and tan δ as a function of temperature. The results in terms of G' and tan δ are presented in Figure 2. At low temperature, PBSA matrix and the corresponding nanocomposites do show a high modulus of order of GPa. PBSA has a low-temperature modulus of about 1.45 GPa. Such a modulus

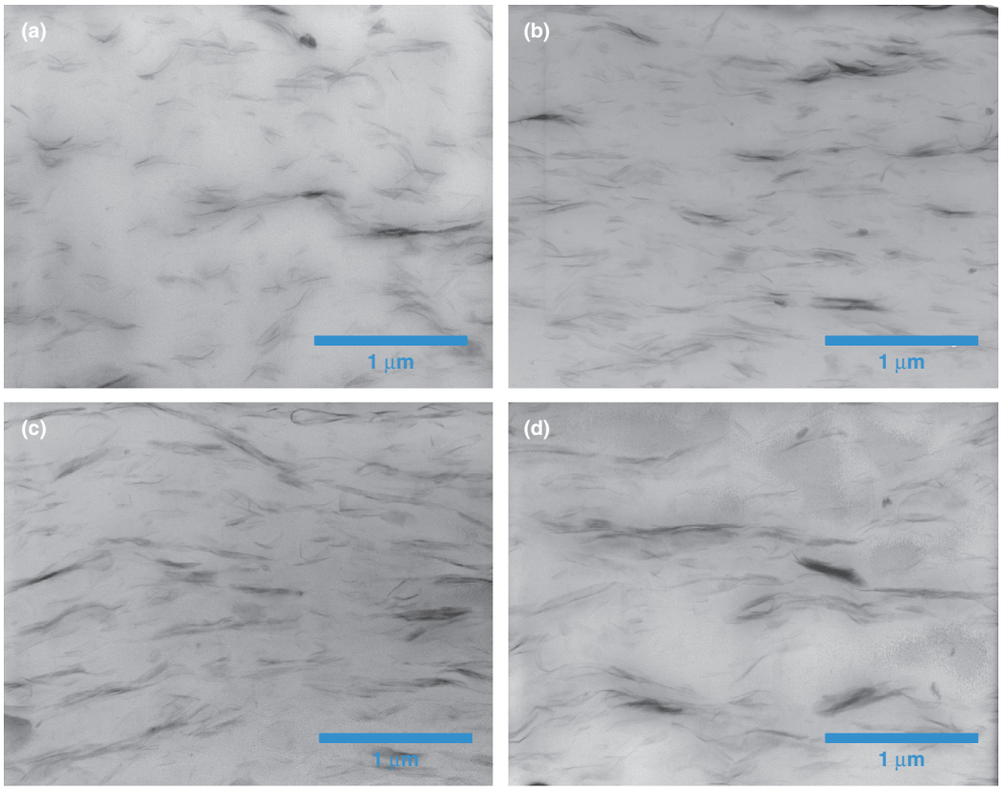

Figure 1. The high-annular-angle-bight-field scanning transmission electron microscopy images of four different model nanocomposite systems, in which bleck entities represent the dispersed clay layers: (a) PBSACN3, (b) PBSACN4, (c) PBSACN5, and (d) PBSACN6. The PBSA nanocomposites with various wt.% of C30B such as 3, 4, 5, 6, were correspondingly abbreviated as PBSACN3, PBSACN4, PBSACN5, and PBSACN6.

increases systematically with increase in C30B loading. At low temperature both PBSA matrix and the PBSACNs are in glassy state. PBSA is characterized by an apparent glass transition temperature (T_g) of about -43 °C that was revealed by a steep decrease in G' followed by a rubbery plateau. The matrix T_g was not affected significantly by C30B incorporation indicating that the relative increase in G' is not due to any modification in T_g, but it is rather related to the degree of dispersion of silicate layers within the PBSA matrix.

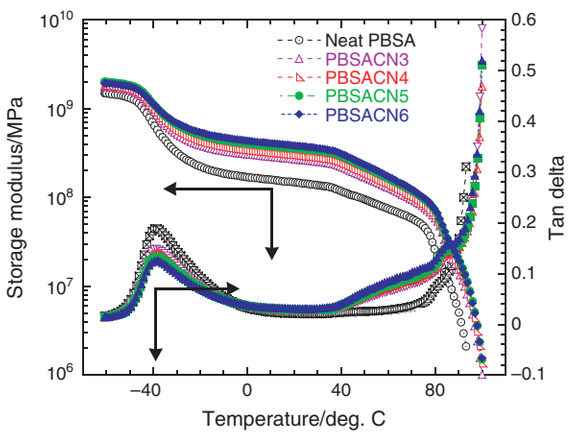

Figure 2. Temperature dependence of storage modulus and tan δ of neat PBSA and various nanocomposites. The PBSA nanocomposites with various wt.% of C30B such as 3, 4, 5, 6, were correspondingly abbreviated asPBSACN3, PBSACN4, PBSACN5, and PBSACN6.

Over the entire measuring temperature range, G' of all PBSACNs is always higher than that of the neat PBSA and systematically increases with increase in C30B loading and this improvement was significant in the case of PBSACN3 as compared to other nanocomposites. This behavior may be due to the high degree of intercalation of polymer chains into the silicate layers of C30B as observed in STEM image, which leads to the large surface area for the interactions between clay and the polymer matrix. Polymer chains inside the silicate galleries are immobilized and the effect of immobilization on the polymers chains may be the main responsible factor for this substantial increase in G'. With increase in C30B loading, clay stacking increases, the flexibility of the samples decreases and they start to behave like solid materials. At room temperature (30 °C), the extent of increase in G' of PBSACN6 is 160% compared to that of neat PBSA.

The melt-state viscoelastic behaviors of nanocomposites are strongly influenced by their nanostructure and the interfacial characteristics. To find out this reversible region, the strain amplitude sweep experiments were performed at

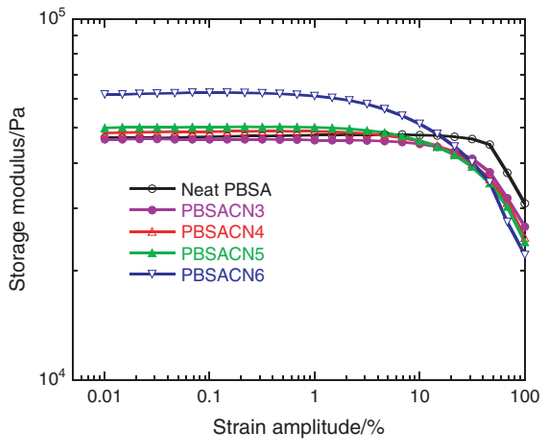

Figure 3. The strain amplitude sweep experiments of neat polymer and various nanocomposite samples at 125 °C with a constant angular frequency, $\omega = 6.28$ rad/s. The PBSA nanocomposites with various wt.% of C30B such as 3, 4, 5, 6, were correspondingly abbreviated as PBSACN3, PBSACN4, PBSACN5, and PBSACN6.

125 °C with a constant angular frequency, $\omega = 6.28$ rad/s in the varying strain of 0.01–100%. The temperature was selected in such a way that there is no degradation of PBSA matrix and the samples are in an isotropic phase. Therefore, any structural change in this state is the result of applied shearing force. As demonstrated in Figure 3 for all samples at low amplitude values in the so-called linear viscoelastic (LVE) region, the G' is showing constant plateau value. At high amplitude values, this LVE region systematically changes with increase in C30B loading. This observation can be attributed to the presence of more and more strain-sensitive rigid network-like structures that are more likely to break down at higher strain-amplitude values, resulting in the narrowing of the region of linear viscoelasticity and the significant increase in G' in the case of PBSACN6. Therefore, the strain chosen for the other oscillatory tests is 0.1%, which makes it possible to study the material behavior of all samples in the LVE region.

Small amplitude oscillatory shear measurements were conducted at a temperature of 125 °C and a strain of 0.1%. The obtained dynamic moduli, G' and G'', are presented in Figure 4 for PBSA and for the corresponding nanocomposites. In the higher frequency region, all samples show $G' > G''$. After a certain frequency ($\sim$1 rad/s) PBSA, PBSACN3 and PBSACN4 show $G' < G''$. For PBSACN5 there is a frequency region where both moduli are overlapping and in the very low frequency region it is nearly approaching a constant limiting value. Further increase in C30B loading results enhance G' more than G'' in the entire frequency range examined with constant limiting value. From the steeply falling nature of G' and G'', especially in the low frequency region, one can say that the neat PBSA, PBSACN3 and PNSACN4 have an unlinked structure, where only mechanical interactions or entanglements

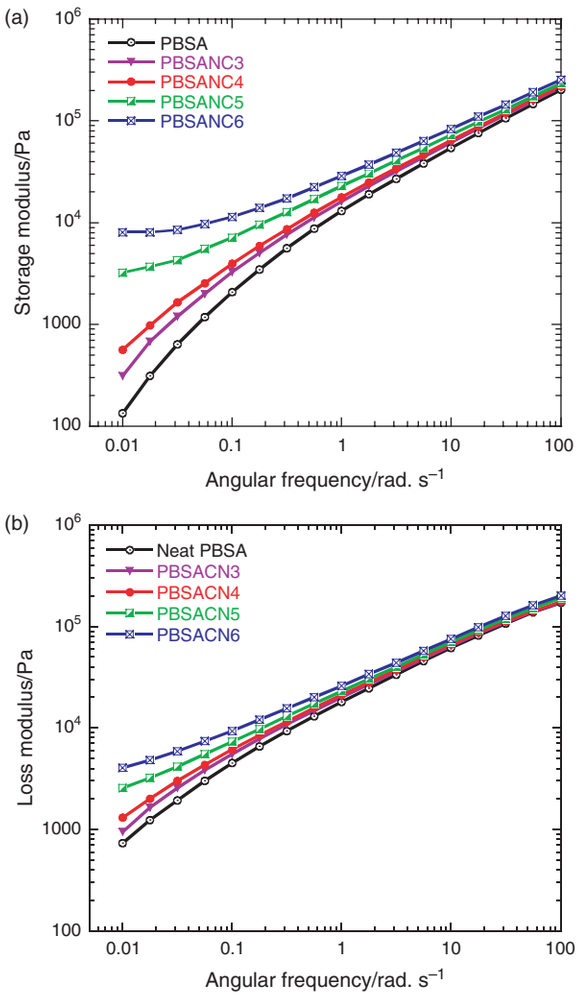

Figure 4. The angular frequency dependence of storage modulus (G') and loss modulus (G'') of neat polymer and various nanocomposite samples. Frequency sweep experiments were conducted at 125 °C with a constant strain value of 0.1%. The PBSA nanocomposites with various wt.% of C30B such as 3, 4, 5, 6, were correspondingly abbreviated as PBSACN3, PBSACN4, PBSACN5, and PBSACN6.

are present. The cross-linking makes it impossible for the polymer chains to glide along each other without destruction of their chemical network. Maximum deformation is possible for widely meshed networks. For a closely packed network system a minimum deformation is permissible and hence in the very low frequency region it is expected that the steeply falling nature of moduli should attain a plateau value. Therefore, it can be confirmed that in the case of PBSACN5 the cross-linking, i.e., the formation of a network between macromolecules that are fixed either by chemical (primary valence bonds forming a chemical network) bonds or by physical–chemical bonds (secondary bonds forming a network of forces) starts. This cross-linking increases with further increase in C30B loading and as a result, G' starts to dominate over G'' in the whole frequency range examined.

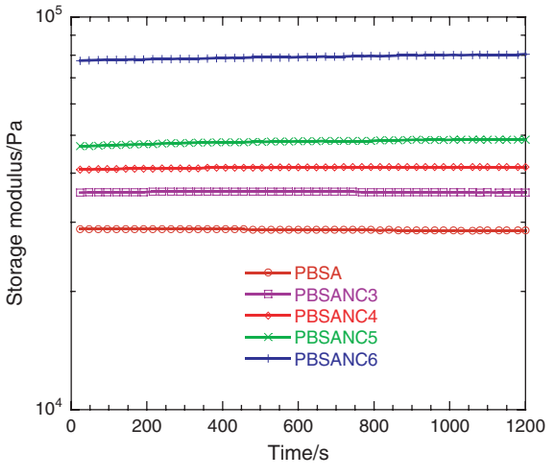

Figure 5. The time dependence of storage modulus (G') of neat polymer and model nanocomposite samples. Time sweep experiments were conducted at 125 °C with a constant strain and frequency value of 0.1% and 6.28 rad/s, respectively. The PBSA nanocomposites with various wt.% of C30B such as 3, 4, 5, 6, were correspondingly abbreviated as PBSACN3, PBSACN4, PBSACN5, and PBSACN6.

To understand the time-dependent behavior of neat PBSA and four different nanocomposites at the experimental temperature, the time sweep experiments were conducted for 1200s at a constant temperature of 125 °C, an applied strain = 0.1% and $\omega = 6.28$ rad/s. The results are summarized in Figure 5. Results showed that the structural strength of all samples remains constant in the examined time interval at 125 °C. The dominant viscous behavior of neat PBSA is getting suppressed up to C30B loading of 4 wt.%. PBSACN5 is showing almost "at the gel point" behavior, suggesting that the material is behaving near the borderline between liquid and solid. On the other hand, PBSACN6 is showing the gel character. This change in properties of nanocomposites with different C30B loadings indicates the formation of different types of network structures of dispersed silicate layers in the PBSA matrix.

4. CONCLUSIONS

Clay-containing nanocomposites of biodegradable PBSA were prepared using melt-mixing and the morphology of dispersed silicate layer was investigated using electron microscopy. The electron microscopy results showed that the amount of organoclay loading plays a vital role in controlling the network structure of dispersed silicate layers of nanocomposites and hence viscoelastic properties.

Acknowledgment: The authors (Shaeel A. Al-Thabaiti, Suprakas Sinha Ray, Sulaiman Nassir Basahel, and Mohamed Mokhtar) would like to thank the Deanship of Scientific Research (DSR), King Abdulaziz University, Jeddah, for financial support (under grant number MG/33/8).

References and Notes

1. R. Ishioka, E. Kitakuni, and Y. Ichikawa, Aliphatic polyesters: Bionolle, biopolymers, polyesters III, Applications and Commercial Products, edited by Y. Doi and A. Steinbuchel, Wiley-VCH, Weinhein **(2002)**, Vol. 4, p. 275.
2. M. S. Nikolic and J. Djonlagic, *Polym. Degrad. Stab.* 74, 263 **(2001)**.
3. T. Fujimaki, *Polym. Degrad. Stab.* 59, 209 **(1998)**.
4. M. Naffakh, C. Marco, M. A. Gómez, G. Ellis, W. K. Maser, A. Benito, and M. T. Martínez, *J. Nanosci. Nanotechnol.* 9, 6120 **(2009)**.
5. Y. S. Yun, H.-R. Pyo, J. Y. Lee, I.-J. Chin, and H.-J. Jin. *J. Nanosci. Nanotechnol.* 13, 7062 **(2013)**.
6. X. Li, Y. Liu, D. Li, and Y. Huang. *J. Nanosci. Nanotechnol.* 13, 5924 **(2013)**.
7. P.-C. Chiu, R. Y.-T. Su, J.-Y. Yeh, C.-Y. Yeh, and R. C.-C. Tsiang, *J. Nanosci. Nanotechnol.* 13, 3910 **(2013)**.
8. G. Kim, S. Kim, S.-Y. Lee, M. Hussain, and Y.-H. Choa, *J. Nanosci. Nanotechnol.* 13, 3936 **(2013)**.
9. J. Lee, Y. S. Yun, D. H. Kim, H. H. Park, and H.-J. Jin, *J. Nanosci. Nanotechnol.* 13, 1769 **(2013)**.
10. M. R. de Moura, F. A. Aouada, L. H. C. Mattoso, and V. Zucolotto, *J. Nanosci. Nanotechnol.* 13, 1946 **(2013)**.
11. Y. Chen, W. Xu, Y. Xiong, C. Peng, W. Liu, G. Zeng, and Y. Peng, *J. Nanosci. Nanotechnol.* 13, 2136 **(2013)**.
12. H. Wang and X. Lai, *J. Nanosci. Nanotechnol.* 13, 1511 **(2013)**.
13. W.-De. Zhang, Y.-M. Zheng, Y.-S. Xu, Y.-X. Yu, Q.-S. Shi, L. Liu, H. Peng, and Y. Ouyang, *J. Nanosci. Nanotechnol.* 13, 409 **(2013)**.
14. H.-J. Kim, Y. Kwon, and C. K. Kim, *J. Nanosci. Nanotechnol.* 13, 577 **(2013)**.
15. L. G. Bach, Md. R. Islam, Y. H. Kim, S. D. Seo, C. Park, H. G. Kim, and K. T. Lim, *J. Nanosci. Nanotechnol.* 13, 694 **(2013)**.
16. S. Sinha Ray, Clay-Containing Polymer Nanocomposites: From Fundamental to Real Applications, Elsevier, Amsterdam **(2013)**.
17. S. Sinha Ray, Environmentally Friendly Polymer Nanocomposites: Types, Processing and Properties, Woodhead Publishing, London **(2013)**.
18. S. Sinha Ray and M. Okamoto, *Prog. Polym. Sci.* 281, 539 **(2003)**.
19. D. R. Paul and L. M. Robeson, *Polymer* 49, 3187 **(2008)**.
20. S. Sinha Ray and M. Bousmina, *Prog. Mater. Sci.* 50, 962 **(2005)**.
21. V. Ojijo and S. Sinha Ray, *Prog. Polym. Sci.* 38, 1543 **(2013)**.
22. S. Sinha Ray and M. Bousmina, *Polymer* 46, 12430 **(2005)**.
23. S. Sinha Ray and M. Bousmina, *Macromol. Mater. Eng.* 290, 759 **(2005)**.
24. S. Sinha Ray, J. Bandyopadhyay, and M. Bousmina, *Polym. Degrad. Stab.* 92, 802 **(2007)**.
25. Very roughly calculated using group contribution method of Fredor, Krevelen DWV, Properties of Polymer, Elsevier, Amsterdam **(1990)**.
26. S. Sinha Ray, *Macromol. Mater. Eng.* 294, 281 **(2009)**.

Received: 30 March 2013. Revised/Accepted: 14 October 2013.